Ultimate Strength Analysis of Reinforced Concrete Cylindrical Containment Shield Walls

J.M. Eidinger, M.A. Manrique
EDS Nuclear Inc.,
220 Montgomery Street, San Francisco, California 94104, U.S.A.

ABSTRACT

The reactor vessel in PWR Nuclear Power Plants is surrounded by a reinforced concrete cylindrical shield wall. This wall must remain integral following a primary loop pipe break LOCA. We have performed analyses of shield walls in eight PWR plants of varying configurations in response to LOCA pressure loads. We have used analytical models incorporating isotropic, orthotropic and nonlinear material models for concrete. There are two load conditions which these walls must resist during the LOCA. First, is the asymmetric blowdown thrust. Second is the uniform pressure loading on the wall. The asymmetric blowdown portion of this loading can be analyzed statically with a Dynamic Load Factor of 1.15. Both load conditions cause similar steel reinforcement stresses near the break location, although detailing requirements differ. Parametric studies show the influence of vertical steel reinforcement on the ultimate capacity of the shield walls. The walls exhibit significant load carrying capacity even after the elastic design limit is surpassed.

1. INTRODUCTION

Recent investigations have shown that original design of nuclear power plants in response to Loss-of-Coolant-Accident (LOCA) conditions may have oversimplified certain loading phenomena. This paper discusses the effects of newly defined LOCA pressure loads on the reinforced concrete cylindrical containment shield walls in Pressurized Water Reactor (PWR) plants. We have analyzed these shield walls up to their ultimate strength because the newer redefined pressure loads on these walls are larger than original design loads. This work has been done to justify to the NRC the safety of operating plants in the United States.

In PWR plants, the reactor vessel is surrounded by a five foot thick cylindrical Biological Shield wall. The wall's function under normal plant operating conditions is to reduce radiation levels in other areas of the Reactor Building. During a LOCA, it must withstand internal pressurization, while maintaining vertical load carrying capacity. A view of the location of the wall with respect to other internal plant structures is shown in Figure 1. As can be seen, there exists several large penetrations in the shield wall, through which pass the 24 inch and 36 inch diameter primary loop piping. The wall is not designed to be a leak-tight pressure retaining boundary.

In the course of our work, we have looked at shield walls in eight different PWRs. No two were identical, nor were they loaded with equal pressures. The parametric study of these various walls and load conditions allow us to present some conclusions as to the behavior of such structures under dynamic load conditions. Further, we will discuss various reinforcement details, and present analytical observations of the ultimate load carrying capacity of cylindrical concrete walls.

2. APPLIED LOADS

Under normal operating conditions, the shield walls are stressed by deadweight and by thermal gradients. The deadweight stress is low. The thermal stress is due to the high operating temperature next to the reactor vessel.

After a LOCA, the shield walls must carry the pressurization within the reactor vessel compartment. The LOCA of concern is caused by a double-ended guillotine pipe break at the reactor vessel nozzle of either the primary inlet or outlet pipes. The suddenly released coolant water flashes to steam and causes rapid pressurization of the annulus space between the reactor vessel and the shield wall. The vents in the shield wall offered by the pipe penetrations allow this pressure to be released into the larger containment building within a few seconds.

Original design of the shield walls assumed that applied LOCA pressures were constant throughout the annulus. This simplified assumption has been questioned by the U. S. Nuclear Regulatory Commission. Detailed thermal hydraulic analyses show that uniform pressure within the annulus is not reached until 0.50 seconds after the pipe break. Immediately after the pipe break, extremely high local pressures exist next to the ruptured pipe, while normal ambient pressures exist in the annulus 180° from the pipe break. This causes an unbalanced, asymmetric net thrust load on the shield walls, not accounted for in the original design.

The spatial time histories of the typical annulus pressures are shown in Figure 2. By integrating these pressure time histories over the surface of the cylindrical shield walls, we get a net asymmetric thrust time history, as shown in Figure 3. The peak magnitude of this thrust can reach as high as 14,000 kips, depending upon the actual pipe break size. As can be seen, the thrust acts as an impulse, peaking at 0.05 seconds; after 0.20 seconds, the thrust is near zero; by 0.50 seconds, a steady-state uniform pressure exists throughout the annulus.

Other loads are occasionally carried by the shield walls. Under seismic events, the walls resist building shears and pipe support reactions. These loads are small in comparison with the LOCA loads. Accident condition temperatures cause self-limiting stresses and experimental evidence shows that the ultimate strength of the shield walls under this condition is not impaired [1].

3. DYNAMIC RESPONSE

The asymmetric portion of the LOCA pressurization is a dynamic loading event. Using several methods, we have investigated the dynamic response of the shield walls. These methods include the following:

1. Axisymmetric Isotropic Models
2. 3-D Isotropic Models
3. 3-D Orthotropic Models

An eigenvalue analysis using the axisymmetric isotropic model of the shield walls yields a first mode frequency of near 40 Hz. Lowest modes are shown in Figure 4. The asymmetric thrust is similar to a triangular load pulse of duration 0.06 to 0.08 seconds. It is, however, almost a slowly applied load to a structure with period 0.025 seconds.

To further investigate the dynamic response of the shield wall, we developed full 3-D models which include major penetrations and major attached boundary walls. One such model is shown in Figure 5. (The EDS Nuclear EDS-SNAP code, based on the ADINA code, was used for analysis.) We performed several dynamic analyses of these models, using the direct integration technique. A damping ratio of 7 percent of critical was used.

The dynamic response of the shield walls is shown in Figure 6. Of the eight PWR plants investigated, the dash line is the response of the stiffest shield wall and the solid line is the response of the softest shield wall.

To insure that these analyses bounded all eight configurations, we used upper and lower bound concrete material property laws. Before significant pressurization, the concrete walls are uncracked; therefore the use of a standard isotropic material law is appropriate. After pressurization, cracks occur due to the high hoop stresses in the cylindrical walls; for this case we used an orthotropic material law. The orthotropic law was set such that the hoop direction stiffness was equal to the equivalent stiffness of hoop steel reinforcement, while the vertical direction stiffness was equal to uncracked concrete properties.

The displacements shown in Figure 6 reveal that the lower bound orthotropic model tends to vibrate more than the upper bound isotropic model. The lower bound model exhibits a vibration frequency of 30 Hz. This frequency reflects a first mode ovalization shape. By comparing static and dynamic analyses of both lower and upper bound stiffness models, we found that little resonance takes place. The static analyses showed almost identical wall displacements and element stresses as did the dynamic analyses.

The reason for the near static/dynamic equivalence is clarified by reviewing the rigorous analysis of one-degree of freedom systems. Adapted from Biggs [2], the DLF spectra for triangular impulse loads is shown in Figure 7. The asymmetric blowdown pulse, from Figure 3, has t_d in the range of 0.06 to 0.08 seconds. The lower and upper bound apparent wall periods are 0.02 and 0.033 seconds, respectively. The t_d/T ratio is therefore between 1.82 and 4.0. Thus, the maximum possible DLF is 1.15, as from Figure 7. This DLF is useful in design of these shield walls for the asymmetric thrust load case. The DLF for the uniform pressure load case is 1.0.

We investigated the load resistance mechanisms as predicted by both the isotropic and orthotropic analyses. Isotropic analysis of reinforced concrete structures predicts accurate hoop direction stresses. Orthotropic analysis, with softer hoop direction stiffness due to cracking of the concrete, predicts a redistribution of load to the edge boundaries of the walls. The wall edge moments and shears due to internal pressurization were in some cases two times larger when calculated by orthotropic rather than by isotropic analysis.

This result is significant in the design of the shield walls. Typically, such walls are designed based on isotropic analysis results [3,4]. If the concrete has indeed cracked, the moment and shear distribution at boundary edges as predicted by isotropic analysis is unconservative.

Detailed stress analysis of the shield walls showed different load carrying mechanisms at the two load conditions.

1. At peak asymmetric thrust, (t=0.05 seconds), the wall distributes load as a two-way shell locally near the pipe break location. High bending moments occur. These moments cause higher tension on the outside layer of hoop steel than the inside layer of hoop steel. The concrete between the penetrations resists load primarily by transferring applied pressure loads into hoop rings directly above or below the penetration level. Large diagonal tension stresses do not occur due to the low one to one aspect ratio of the concrete sections in this area.
2. At steady state pressurization, (t=0.50 seconds), the walls behave as uniformly pressurized concrete tanks. The high local bending moments due to peak asymmetric thrust are replaced with high hoop tensions due to steady-state pressurization. Highest hoop tension loads occur on the inside layer of hoop steel.

4. ULTIMATE STRENGTH ANALYSIS

The ultimate strength behavior of the primary shield walls is evaluated by performing a nonlinear analysis on the axisymmetric finite element model shown in Figure 8. This model uses the nonlinear concrete material law available in the ADINA code [5]. Eight node axisymmetric elements are used to represent the concrete. The hoop and vertical reinforcement are included in the form of one-node ring and three-node truss elements, respectively. The strength of the concrete is taken at 6650 psi in compression and 460 psi in tension. The reinforcement is modeled on an elastoplastic, strain hardening material. Yield stress of 45,000 psi and ultimate stress of 73,000 psi are used. The main portion of the shield wall is 5 feet thick, has an inside radius of 11.5 feet, and is 23 feet tall.

An incremental solution is adoped to solve the nonlinear problem. Stiffness reformation is performed at each load increment. Smaller load increments are prescribed when entering the nonlinear region, when the conrete begins to crack.

Three different ratios of vertical reinforcement (ρ) are used in the analysis performed on the finite element model:

Case 1:	No vertical reinforcement: $\rho = 0.0$
Case 2:	Vertical reinforcement ratio of $\rho = 0.63\%$
Case 3:	Vertical reinforcement ratio of $\rho = 1.26\%$

The hoop reinforcement ratio is $\rho = 1.23\%$ for all three cases. Based upon full yield of all hoop reinforcement, the design pressure load is 177 psi.

Figure 9 is a plot of maximum radial displacements of the shield wall due to internal pressure loading. The response is described in four ranges.

Range 1.	Elastic
Range 2.	Concrete cracks, steel elastic.
Range 3.	Concrete cracked, hoop steel yielding, vertical steel elastic.
Range 4.	Concrete cracked, hoop and vertical steel yielded.

The response is very similar in the linear Range 1 for the three cases. Bending stresses at the pedestal/shield wall juncture (see Figure 1 for location) induce first cracking of the conrete at a pressure of about 130 psi.

In Range 2, significant radial cracking of the concrete due to hoop stress spreads across the wall. This is accompanied by a rapid deterioration of the wall stiffness. This in turn induces first yielding of the hoop reinforcement at an internal pressure of about 150 psi.

From this point onwards, the effect of the vertical reinforcement increases noticeably. In Range 3, the cases with vertical reinforcement depict an increase in overall stiffness due to a decrease in the rate of concrete cracking. Further, the redistribution of stresses as a result of the two way slab action induced by the vertical reinforcement restrains unlimited radial displacement of the wall. The lack of vertical reinforcement in Case 1 causes rapid yielding of the hoop reinforcement and further deterioration of the shield wall stiffness. As the applied load increases, yielding of the vertical reinforcement occurs at the location where cracks due to bending stresses first appeared. The internal pressure at first vertical steel yeild is 190 psi for Case 2 and 225 psi for Case 3.

In Range 4, yielding of the vertical reinforcement spreads to the outside face of the wall. The internal pressure at this point is 215 psi for Case 2 and 240 psi for Case 3.

Only the models with vertical reinforcement are able to withstand significant further internal pressurization in the fully nonlinear Range 4. In this Range, the hoop steel yields throughout most of the height of the wall. As this occurs, the vertical reinforcement redistributes the loads to less stressed regions.

The key result is that vertical reinforcement provides significant overload capacity to these cylindrical concrete walls. For the model analyzed, the design load based on hoop steel strength is 177 psi. By considering vertical steel reinforcement, an over-strength capacity of more than 50 percent is shown. These results are given in Table I.

5. SUMMARY

We have performed analyses of concrete containment shield walls in response to LOCA pressure loads. The loads were found to be described in two phases. First, there is an asymmetric thrust load on the walls. Second, there is a uniform steady state pressure load on the walls. DLFs corresponding to these loads of 1.15 and 1.0, respectively, account for dynamic effects.

The following key observations are made:

1. The vertical reinforcement of the shield wall plays a significant role in the ultimate strength behavior of the structure.
   - At overload conditions, the presence of moderate amounts of vertical steel induces two way slab action, allowing the structure to withstand as much as 150% of elastic basis design load.
2. Cracking of the concrete with subsequent reduction of hoop direction stiffness leads to higher bending moments and shear forces at the boundaries of the wall than predicted by elastic isotropic analysis.
3. The design of the shield walls for the asymmetric portion of the load requires special considerations.
   - The amount of hoop reinforcement should be equal at both the inside and outside faces of the wall. However, the steady-state pressure will typically control the total amount of hoop steel required.

6. REFERENCES

[1] Y. Aoyagi, et al., "Behavior of Reinforced Concrete Containment Models Under Thermal Gradient and Internal Pressure", Proceedings 5th Intl Conference of Structural Mechanics in Reactor Technology, Berlin, 1979.

[2] J. M. Biggs, Introduction to Structural Dynamics, New York: McGraw-Hill Book Co., 1974.

[3] Circular Tanks Without Prestressing, Portland Cement Association, No. ST 57.

[4] Structrual Analysis and Design of Nuclear Plant Facilities. Draft Trial Use and Comment. Prepared by the Editing Board and Task Groups of the Committee on Nuclear Structures and Materials of the Structural Division of the ASCE, 1976.

[5[K. J. Bathe, and S. Ramaswamy, "On Three Dimensional Nonlinear Analysis of Concrete Structures", Nuclear Engineering and Design, Vol. 52, pp 385-409, 1979.

TABLE I - SUMMARY ULTIMATE STRENGTH OF WALLS

Case	Vertical Reinforcement Ratio	Actual Pressure (psi)	Maximum Lateral Deflection (inch)	Maximum Strain In Hoop Reinforcement	Actual Pressure / Design Pressure (Note 1)
Case 1	0.0	232	3.2	2.1%	1.31
Case 2	0.63%	232	1.7	1.2%	1.31
Case 3	1.26%	232	0.9	0.6%	1.31
Case 2	0.63%	280	4.6	3.1%	1.58
Case 3	1.26%	280	2.6	1.7%	1.58

(1) Design pressure = 177 psi. See text.

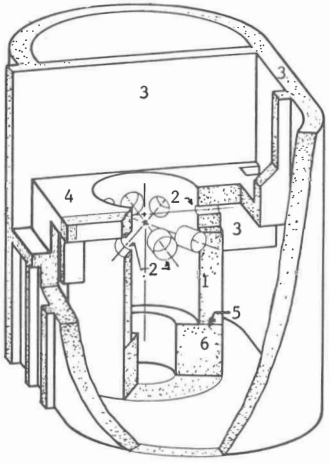

Item

1. Biological Shield Wall
2. Pipe Penetrations
3. Other Walls
4. Other Floor
5. Pedestal/ Shield Wall Interface
6. Pedestal

Fig. 1. Shield Wall and Interior Structures

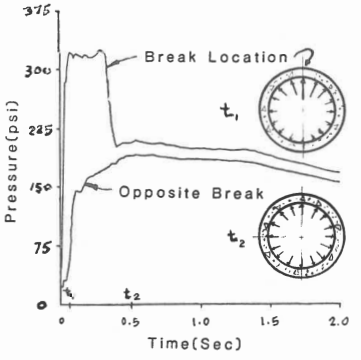

Fig. 2. Shield Wall Pressures

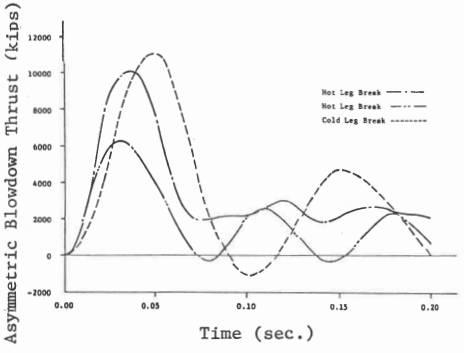

Fig. 3. Asymmetric Blowdown Thrust

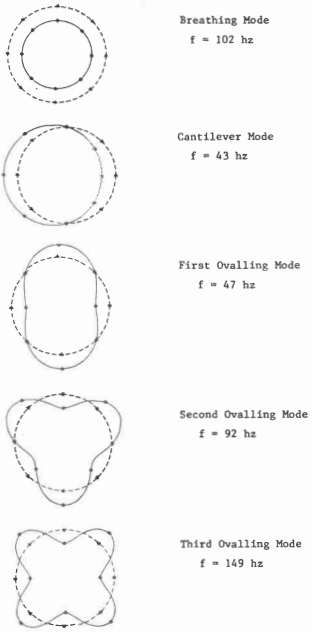

Fig. 4. Isotropic Mode Shapes

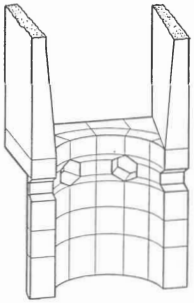

Fig. 5. 3-D Shield Wall Model (Half Shown)

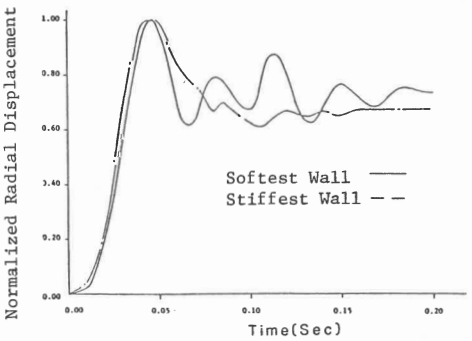

Fig. 6. Shield Wall Dynamic Response

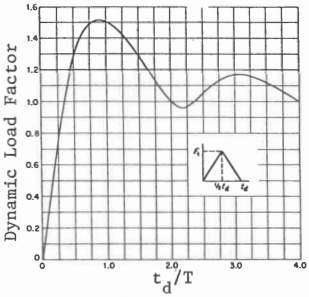

Fig. 7. DLF for Impulse Load

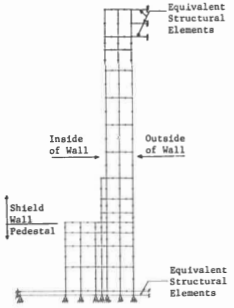

Fig. 8. Nonlinear Shield Wall Model (Elevation)

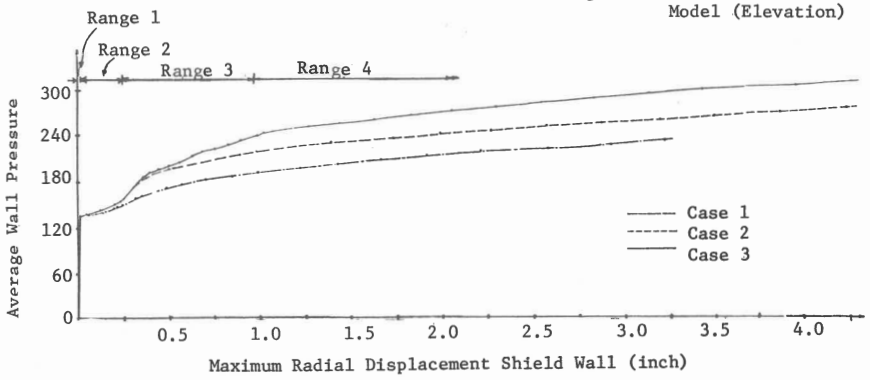

Fig. 9. Nonlinear Shield Wall Response